Bibliography

[1] ABB Automation (2000), *Specification: Variable Area Flowmeters – Series 10A6100*.

[2] Ahn, C., Akamatsu, F., Katsuki, M. and Kitajima, A. (2003), The influences of mixture composition and preheat temperature on combustion regime and flame structure of premixed turbulent flames, 'The Fourth Asia-Pacific Conference on Combustion', pp. 40–43.

[3] Angrill, O., Geitlinger, H., Streibel, T., Suntz, R. and Bockhorn, H. (2000), Influence of exhaust gas recirculation on soot formation in diffusion flames, 'Proceedings of the Combustion Institute', Vol. 28, pp. 2643–2649.

[4] Atkins, P. W. (1983), *Molecular Quantum Mechanics*, 2nd Edn, Oxford University Press.

[5] Banwell, C. (1966), *Fundamentals of Molecular Spectroscopy*, McGraw-Hill Publishing Company Limited.

[6] Barlow, R. S. and Carter, C. D. (1994), 'Raman/Rayleigh/LIF Measurements of Nitric Oxide Formation in Turbulent Hydrogen Jet Flames', *Combustion and Flame* **97**, 261–280.

[7] Barlow, R. S., Fiechtner, G. J., Carter, C. D. and Chen, J.-Y. (2000), 'Experiments on the Scalar Structure of Turbulent $CO/H_2/N_2$ Jet Flames', *Combustion and Flame* **120**, 549–569.

[8] Barlow, R. S., Karpetis, A. N., Frank, J. H. and Chen, J.-Y. (2001), 'Scalar Profiles and NO Formation in Laminar Opposed-Flow Partially Premixed Methane/Air Flames', *Combustion and Flame* **127**, 2102–2118.

[9] Bengtsson, P.-E. (1996), 'Simultaneous Two-Dimensional Visualization of Soot and OH in Flames Using Laser-Induced Fluorescence', *Applied Spectroscopy* **50**(9), 1182–1186.

[10] Berg, P. A., Hill, D. A., Noble, A. R., Smith, G. P., Jeffries, J. B. and Crosley, D. R. (2000), 'Absolute CH Concentration Measurements in Low-Pressure Methane Flames: Comparisons with Model Results', *Combustion and Flame* **121**, 223–235.

[11] Bergmann, V., Meier, W., Wolff, D. and Stricker, W. (1998), 'Application of spontaneous Raman and Rayleigh scattering and 2D LIF for the characterization of a turbulent $CH_4/H_2/N_2$ jet diffusion flame', *Applied Physics B* **66**, 489–502.

[12] Bijjula, K. and Kyritsis, D. C. (2005), Experimental evaulation of flame observables for simplified scalar dissipation rate measurements in laminar diffusion flamelets, 'Proceedings of the Combustion Institute', Vol. 30, pp. 493–500.

[13] Bilger, R. W. (1988), The structure of turbulent nonpremixed flames, 'Proceedings of the Combustion Institute', Vol. 28, pp. 475–488.

[14] Bombach, R. and Käppeli, B. (1999), 'Simultaneous visualisation of transient species in flames by planar-laser-induced fluorescence using a single laser system', *Applied Physics B* **68**, 251–255.

[15] Borman, G. L. and Ragland, K. W. (1998), *Combustion Engineering*, International Ed^{n}, The McGraw-Hill Companies, Inc.

[16] Brockhinke, A., Haufe, S. and Kohse-Höinghaus, K. (2000), 'Structural Properties of Lifted Hydrogen Jet Flames Measured by Laser Spectroscopic Techniques', *Combustion and Flame* **121**, 367–377.

[17] Buch, K. A., Dahm, W. J. A., Dibble, R. W. and Barlow, R. S. (1992), Structure of equilibrium reaction rate fields in turbulent jet diffusion flames, 'Proceedings of the Combustion Institute', Vol. 24, pp. 295–301.

[18] Burggraaf, B. T., Lewis, B., Hoppesteyn, P. D. J., Fricker, N., Santos, S. and Slim, B. K. (2005), Towards industrial application of high efficiency combustion, Research Digest IFRF Doc. No. K70/y/156, International Flame Research Foundation.

[19] Burkert, A., Grebner, D., Müller, D., Triebel, W. and König, J. (2000), Single-shot Imaging of formaldehyde in hydrocarbon flames by XeF Excimer Laser-Induced Fluorescence, 'Proceedings of the Combustion Institute', Vol. 28, pp. 1655–1661.

[20] Cabra, R., Chen, J.-Y., Dibble, R. W., Karpetis, A. N. and Barlow, R. S. (2005), 'Lifted methane-air jet flames in a vitiated coflow', *Combustion and Flame* **143**, 491–506.

[21] Cabra, R., Myhrvold, T., Chen, J. Y., Dibble, R. W., Karpetis, A. N. and Barlow, R. S. (2002), Simultaneous laser Raman-Rayleigh-LIF measurements and numerical modelling results of a lifted turbulent H_2/N_2 jet flame in a vitiated coflow, 'Proceedings of the Combustion Institute', Vol. 29, pp. 1881–1888.

[22] Cao, R. R., Pope, S. B. and Masri, A. R. (2005), 'Turbulent lifted flames in a vitiated coflow investigated using joint PDF calculations', *Combustion and Flame* **142**, 438–453.

[23] Carter, C. D. and Barlow, R. S. (1994), 'Simultaneous measurements of NO, OH, and the major species in turbulent flames', *Optics Letters* **19**(4), 299–301.

[24] Cavaliere, A. and de Joannon, M. (2004), 'Mild combustion', *Progress in Energy and Combustion Science* **30**, 329–366.

[25] Chen, A. K. and Polik, W. F. (1996), 'K-Rotational Relaxation of S_1 H_2CO ($v_4 = 1, J_{K_aK_c} = 1_{01}$) via Dispersed Fluorescence Spectroscopy', *Journal of Physical Chemistry* **100**, 10027–10036.

[26] Chigier, N. (1981), *Energy, Combustion, and Environment*, McGraw-Hill Book Company.

[27] Choi, G.-M. and Katuski, M. (2001), 'Advanced low NO_x combustion using highly preheated air', *Energy Conversion and Management* **42**, 639–652.

[28] Christo, F. C. and Dally, B. B. (2005), 'Modeling turbulent reacting jets issuing into a hot and diluted coflow', *Combustion and Flame* **142**, 117–129.

[29] Coelho, P. J. and Peters, N. (2001), 'Numerical simulation of a mild combustion burner', *Combustion and Flame* **124**, 503–518.

[30] Dally, B. B., Karpetis, A. N. and Barlow, R. S. (2002*a*), Structure of Jet Laminar Nonpremixed Flames under Diluted Hot Coflow Conditions, '2002 Australian Symposium on Combustion and The Seventh Australian Flame Days', Adelaide, Australia.

[31] Dally, B. B., Karpetis, A. N. and Barlow, R. S. (2002*b*), Structure of turbulent non-premixed jet flames in a diluted hot coflow, 'Proceedings of the Combustion Institute', Vol. 29, pp. 1147–1154.

[32] Dally, B. B., Riesmeier, E. and Peters, N. (2004), 'Effect of fuel mixture on moderate and intense low oxygen dilution combustion', *Combustion and Flame* **137**, 418–431.

[33] Dally, B. and Peters, N. (2002), Effect of Fuel Mixture on MILD Combustion. Work done during sabbatical at ITM in 2002.

[34] de Joannon, M., Saponaro, A. and Cavaliere, A. (2000), Zero-dimensional analysis of diluted oxidation of methane in rich conditions, 'Proceedings of the Combustion Institute', Vol. 28, pp. 1639–1646.

[35] de Vries, J. (1994), Study on turbulent fluctuations in diffusion flames using laser induced fluorescence, PhD thesis, Delft University of Technology.

[36] Dibble, R. W. and Hollenbach, R. E. (1981), Laser Rayleigh Thermometry in Turbulent Flames, 'Proceedings of the Combustion Institute', Vol. 18, pp. 1489–1499.

[37] Dieke, G. H. and Crosswhite, H. M. (1962), 'The Ultraviolet Bands of OH', *Journal of Quantitative Spectroscopy and Radiative Transfer* **2**, 97–199.

[38] Dieke, G. H. and Kistiakowsky, G. B. (1934), 'The structure of the ultraviolet absorption spectrum of formaldehyde. I', *Physical Review* **45**, 4–28.

[39] Donbar, J. M., Driscoll, J. F. and Carter, C. D. (2000), 'Reaction Zone Structure in Turbulent Nonpremixed Jet Flames – From CH-OH PLIF Images', *Combustion and Flame* **122**, 1–19.

[40] Du, J. and Axelbaum, R. L. (1995), 'The effect of flame structure on soot-particle inception in diffusion flames', *Combustion and Flame* **100**, 367–375.

[41] Eckbreth, A. C. (1996), *Laser Diagnostics For Combustion Temperature and Species*, Gordon and Breach Publishers.

[42] Emery, C. D., Overway, K. S., Bouwens, R. J. and Polik, W. F. (1995), 'Dispersed fluorescence spectroscopy of excited rovibrational states in S_0 formaldehyde', *Journal of Chemical Physics* **103**(13), 5279–5289.

[43] Energy Information Administration (2003), International Energy Outlook 2003, DOE/EIA-0484(2003), U.S. Department of Energy.

[44] Gardiner Jr, W. C. (1984), *Combustion Chemistry*, Springer-Verlag New York Inc.

[45] Garland, N. L. and Crosley, D. R. (1986), On the collisional quenching of electronically excited OH, NH and CH in flames, 'Proceedings of the Combustion Institute', Vol. 21, pp. 1693–1702.

[46] Gkagkas, K. and Lindstedt, R. P. (2007), Transported PDF modelling with detailed chemistry of pre- and auto-ignition in CH_4/air mixtures, 'Proceedings of the Combustion Institute', Vol. 31, pp. 1559–1566.

[47] Gordon, R. L., Dunn, M. J., Masri, A. R. and Bilger, R. W. (2005), Joint Imaging of Rayleigh and LIF-OH at the Base of Lifted Flames Issuing in Vitiated Coflow, 'Fourth Australian Conference on Laser Diagnostics in Fluid Mechanics and Combustion', The University of Adelaide, South Australia, Australia, pp. 45–48.

[48] Gordon, R. L., Stårner, S. H., Masri, A. R. and Bilger, R. W. (2005), Further characterisation of lifted hydrogen and methane flames issuing into a

vitiated coflow, '5th Asia-Pacific Conference on Combustion', The University of Adelaide, Adelaide, Australia, pp. 333–336.

[49] Guo, H., Ju, Y., Maruta, K. and Niioka, T. (1997), 'Radiaton extinction limit of counterflow premixed lean methane-air flames', *Combustion and Flame* **109**, 639–646.

[50] Guo, H., Liu, F., Smallwood, G. J. and Gülder, Ö. L. (2006), 'Numerical study on the influence of hydrogen addition on soot formation in a laminar ethylene-air diffusion flame', *Combustion and Flame* **145**, 324–338.

[51] Han, D. and Mungal, M. G. (2001), 'Direct Measurement of Entrainment in Reacting/Nonreacting Turbulent Jets', *Combustion and Flame* **124**, 370–386.

[52] Harrington, J. E. and Smyth, K. C. (1993), 'Laser-induced fluorescence measurements of formaldehyde in a methane/air diffusion flame', *Chemical Physics Letters* **202**, 196–202.

[53] Hasegawa, T., Tanaka, R. and Niioka, T. (1997), Combustion with high temperature low oxygen air in regenerative burners, 'The First Asia-Pacific Conference on Combustion', Osaka, Japan, pp. 290–293.

[54] Im, H. G. and Chen, J. H. (1999), 'Structure and propagation of triple flames in partially premixed hydrogen-air mixtures', *Combustion and Flame* **119**, 436–454.

[55] Im, H. G., Chen, J. H. and Chen, J.-Y. (1999), 'Chemical Response of Methane/Air Diffusion Flames to Unsteady Strain Rate', *Combustion and Flame* **118**, 204–212.

[56] Ishiguro, T., Tsuge, S., Furuhata, T., Kitagawa, K., Arai, N., Hasegawa, T., Tanaka, R. and Gupta, A. K. (1998), Homogenization and stabilization during combustion of hydrocarbons with preheated air, 'Proceedings of the Combustion Institute', Vol. 27, pp. 3205–3213.

[57] Joedicke, A., Peters, N. and Mansour, M. (2005), The stabilization mechanism and structure of turbulent hydrocarbon lifted flames, 'Proceedings of the Combustion Institute', Vol. 30, pp. 901–909.

[58] Katsuki, M. and Hasegawa, T. (1998), The science and technology of combustion in highly preheated air combustion, 'Proceedings of the Combustion Institute', Vol. 27, pp. 3135–3146.

[59] Kelman, J. B. and Masri, A. R. (1997*a*), 'Quantitative technique for imaging mixture fraction, temperature, and the hydroxyl radical in turbulent diffusion flames', *Applied Optics* **36**(15), 3506–3514.

[60] Kelman, J. B. and Masri, A. R. (1997*b*), 'Reaction zone structure and scalar dissipation rates in turbulent diffusion flames', *Combustion Science and Technology* **129**, 17–55.

[61] Kim, S. H., Huh, K. Y. and Dally, B. (2005), Conditional moment closure modeling of turbulent nonpremixed combustion in diluted hot coflow, 'Proceedings of the Combustion Institute', Vol. 30, pp. 751–757.

[62] King, G. F., Dutton, J. C. and Lucht, R. P. (1999), 'Instantaneous, quantitative measurements of molecular mixing in the axisymmetric jet near field', *Physics of Fluids* **11**(2), 403–416.

[63] Klein-Douwel, R. J. H., Luque, J., Jeffries, J. B., Smith, G. and D.R., C. (1999), CH and CH_2O in Atmospheric Pressure Methane/Air Bunsen Flames, 'Western States Section of the Combustion Institute (USA)'. Paper 12F99.

[64] Klein-Douwel, R. J. H., Luque, J., Jeffries, J. B., Smith, G. P. and Crosley, D. R. (2000), 'Laser-induced fluorescence of formaldehyde hot bands in flames', *Applied Optics* **39**(21), 3712–3715.

[65] Kohse-Höinghaus, K. and Jeffries, J. B. (2002), *Applied Combustion Diagnostics*, Taylor & Francis.

[66] Kumar, S., Paul, P. J. and Mukunda, H. S. (2002), Studies on a new high-intensity low-emission burner, 'Proceedings of the Combustion Institute', Vol. 29, pp. 1131–1137.

[67] Luque, J. and Crosley, D. R. (1999), LIFBASE: Database and Spectral Simulation Program, Report MP 99-009, SRI International.

[68] Luque, J., Jeffries, J. B., Smith, G. P. and Crosley, D. R. (2001), 'Quasi-simultanous detection of CH_2O and CH by cavity ring-down absorption and laser-induced fluorescence in a methane/air low-pressure flame', *Applied Physics B* **73**, 731–738.

[69] Luque, J., Klein-Douwel, R. J. H., Jeffries, J. B., Smith, G. P. and Crosley, D. R. (2001), Measurement of CH_2O in low and atmospheric pressure flames by laser induced fluorescence and cavity ringdown absorbtion, '2^{nd} Joint Meeting of the US sections of the Combustion Institute (USA)'.

[70] Maessen, B. and Wolfsberg, M. (1984), 'Variational calculation of lower vibrational energy levels of formaldehyde $\tilde{X}^1A_1$', *Journal of Chemical Physics* **80**(10), 4651–4662.

[71] Mancini, M., Weber, R. and Bollettini, U. (2002), Predicting NO_x emissions of a burner operated in flameless oxidation mode, 'Proceedings of the Combustion Institute', Vol. 29, pp. 1155–1163.

[72] Mansour, M. S. (2003), 'Stability characteristics of lifted turbulent partially premixed jet flames', *Combustion and Flame* **133**, 263–274.

[73] Maruta, K., Muso, K., Takeda, K. and Niioka, T. (2000), Reaction zone structure in flameless combustion, 'Proceedings of the Combustion Institute', Vol. 28, pp. 2117–2123.

[74] Masri, A. R., Dibble, R. W. and Barlow, R. S. (1996), 'The structure of turbulent nonpremixed flames revealed by Raman-Rayleigh-LIF measurements', *Progress In Energy and Combustion Science* **22**, 307–362.

[75] Masri, A. R., Kelman, J. B. and Dally, B. B. (1998), The Instantaneous Spatial Structure Of The Recirculation Zone In Bluff-Body Stabilized Flames, 'Proceedings of the Combustion Institute', Vol. 28, pp. 1031–1038.

[76] Mastorakos, E., Taylor, A. M. K. P. and Whitelaw, J. H. (1995), 'Extinction of turbulent counterflow flames with reactants diluted by hot products', *Combustion and Flame* **102**, 101–114.

[77] Mc Enally, C. S. and Pfefferle, L. D. (2000), 'Experimental study of nonfuel hydrocarbons and soot in coflowing partially premixed ethylene/air flames', *Combustion and Flame* **121**, 575–592.

[78] McEnally, C. S. and Pfefferle, L. D. (1999), 'Experimental Study of Nonfuel Hydrocarbon Concentrations in Coflowing Partially Premixed Methane/Air Flames', *Combustion and Flame* **118**, 619–632.

[79] Mi, J., Nobes, D. S. and Nathan, G. J. (2001), 'Influence of jet exit conditions on the passive scalar field of an axisymmetric free jet', *Journal of Fluid Mechanics* **432**, 91–125.

[80] Milani, A. and Saponaro, A. (2001), Diluted combustion technologies, Article Number 200101, IFRF Combustion Journal.

[81] Muñiz, L. and Mungal, M. G. (2001), 'Effects of Heat Release and Buoyancy on Flow Structure and Entrainment In Turbulent Nonpremixed Flames', *Combustion and Flame* **126**, 1402–1420.

[82] Müller, H. S. P., Winnewisser, G., Demaison, J., Perrin, A. and Valentin, A. (2000), 'The ground state spectroscopic constants of formaldehyde', *Journal of Molecular Spectroscopy* **200**, 143–144.

[83] Murphy, J. S. and Boggs, J. E. (1969), 'Collisional Broadening of Rotational Absorption Lines. V. Pressure Broadening of Microwave Absorption Spectra Involing Asymmetric-Top Molecules', *The Journal of Chemical Physics* **51**(9), 3891–3901.

[84] Najm, H. N., Knio, O. M., Paul, P. H. and Wyckoff, P. S. (1998), 'A study of flame observables in premixed methane-air flames', *Combustion Science and Technology* **140**, 369–403.

[85] Najm, H. N., Paul, P. H., Mueller, C. J. and Wyckoff, P. S. (1998), 'On the adequacy of certain experimental observables as measurements of flame burning rate', *Combustion and Flame* **113**, 312–332.

[86] Namer, I. and Schefer, R. W. (1985), 'Error estimates for Rayleigh scattering density and temperature measurements in premixed flames', *Experiments in Fluids* **3**, 1–9.

[87] Nishimura, M., Suzuki, T., Nakanishi, R. and Kitamura, R. (1997), 'Low-NO_x combustion under highly preheated air temperature condition in an industrial furnace', *Energy Conversion and Management* **38**, 1353–1363.

[88] Özdemir, I. B. and Peters, N. (2001), 'Characteristics of the reaction zone in a combustor operating at MILD combustion', *Experiments In Fluids* **30**, 683–695.

[89] Paul, P. H. (1995), 'Vibrational Energy Transfer and Quenching of OH $A^2\Sigma^+(v' = 1)$ Measured at High Temperatures in a Shock Tube', *Journal of Physical Chemistry* **99**, 8472–8476.

[90] Paul, P. H., Carter, C. D., Gray, J. A., Durant Jr., J. L. and Furlanetto, M. R. (1994), Correlations for the OH $A^2\Sigma^+$ $(v' = 0)$ Electronic Quenching Cross-section, SAND94-8244, Sandia National Laboratories.

[91] Paul, P. H. and Najm, H. N. (1998), Planar laser-induced fluorescence imaging of flame heat release rate, 'Proceedings of the Combustion Institute', Vol. 27, pp. 43–50.

[92] Pitsch, H. and Steiner, H. (2000), Scalar mixing and dissipation rate in large-eddy simulations of non-premixed turbulent combustion, 'Proceedings of the Combustion Institute', Vol. 28, pp. 41–49.

[93] Pitts, W. M., Richards, C. D. and Levenson, M. S. (1999), Large- and Small-Scale Structures and Their Interactions in an Axisymmetric Jet, NISTIR 6393, National Institute of Standards and Technology.

[94] Plessing, T., Peters, N. and Wünning, J. G. (1998), Laseroptical investigation of highly preheated combustion with strong exhaust gas recirculation, 'Proceedings of the Combustion Institute', Vol. 27, pp. 3197–3204.

[95] Plessing, T., Terhoeven, P., Peters, N. and Mansour, M. S. (1998), 'An experimental and numerical study of a laminar triple flame', *Combustion and Flame* **115**, 335–353.

[96] Pope, S. B. (2000), *Turbulent Flows*, First Ed$^{\underline{n}}$, Cambridge University Press.

[97] Ranzi, E., Dente, M., Goldaniga, A., Bozzano, G. and Faravelli, T. (2001), 'Lumping procedures in detailed kinetic modeling of gasification, pyrolysis, partial oxidation and combustion of hydrocarbon mixtures', *Progress in Energy and Combustion Science* **27**, 99–139.

[98] Reaction Design (2001), OPPDIF: A Program for Computing Opposed-Flow Diffusion Flames, User Manual OPP-036-2.

[99] Refael, S. and Sher, E. (1989), 'Reaction Kinetics of Hydrogen-Enriched Methane-Air and Propane-Air Flames', *Combustion and Flame* **78**, 326–338.

[100] Renfro, M. W., Guttenfelder, W. A., King, G. B. and Laurendeau, N. M. (2000), 'Scalar Time-Series Measurements in Turbulent $CH_4/H_2/N_2$ Non-premixed Flames: OH', *Combustion and Flame* **123**, 389–401.

[101] Rensberger, K. J., Jeffries, J. B., Copeland, R. A., Kohse-Höinghaus, K., Wise, M. L. and Crosley, D. R. (1989), 'Laser-induced fluorescence determination of temperatures in low pressure flames', *Applied Optics* **28**(17), 3556–3566.

[102] Røkke, N. A., Hustad, J. E. and Sønju, O. K. (1994), 'A Study of Partially Premixed Unconfined Propane Flames', *Combustion and Flame* **97**, 88–106.

[103] Shin, D. I., Dreier, T. and Wolfrum, J. (2001), 'Spatially resolved absolute concentration and fluorescence-lifetime determination of H_2CO in atmospheric-pressure CH_4/air flames', *Applied Physics B* **72**, 257–261.

[104] Stårner, S. H., Bilger, R. W., Dibble, R. W. and Barlow, R. S. (1990), 'Piloted diffusion flames of diluted methane near extinction: Detailed structure from laser measurements', *Combustion Science and Technology* **72**, 255–269.

[105] Stepowski, D. and Cabot, G. (1992), 'Single-Shot Temperature and Mixture Fraction Profiles by Rayeleigh Scattering in the Development Zone of a Turbulent Diffusion Flame', *Combustion and Flame* **88**, 296–308.

[106] Sun, C. J., Sung, C. J., Wang, H. and Law, C. K. (1996), 'On the structure of nonsooting counterflow ethylene and acetylene diffusion flames', *Combustion and Flame* **107**, 321–335.

[107] Szegö, G. G., Dally, B. B., Nathan, G. J. and Christo, F. C. (2007), Performance Characteristics of a 20kW MILD Combustion Furnace, '6$^{\text{th}}$ Asia-Pacific Conference on Combustion', Nagoya, Japan, pp. 231–234.

[108] Tacke, M. M., Geyer, D., Hassel, E. P. and Janicka, J. (1998), A detailed investigation of the stabilization point of lifted turbulent diffusion flames, 'Proceedings of the Combustion Institute', Vol. 27, pp. 1157–1165.

[109] *The Pocket Oxford Dictionary* (1946), Fourth (revised) Ed$^{\underline{\text{n}}}$, Oxford University Press.

[110] Tolocka, M. P. and Miller, J. H. (1998), Measurements of formaldehyde concentrations and formation rates in a methane-air, non-premixed flame and their implications for heat-release, 'Proceedings of the Combustion Institute', Vol. 27, pp. 633–640.

[111] Turns, S. (2000), *An Introduction to Combustion: Concepts and Applications*, 2$^{\text{nd}}$ Ed$^{\underline{\text{n}}}$, McGraw-Hill Publishing Company Limited.

[112] Upatnieks, A., Driscoll, J. F. and Ceccio, S. L. (2002), Cinema particle imaging velocimetry time history of the propagation velocity of the base of a lifted turbulent jet flame, 'Proceedings of the Combustion Institute', Vol. 29, pp. 1897–1903.

[113] Weber, R., Orsino, S., Lallemant, N. and Verlaan, A. (2000), Combustion of natural gas with high-temperature air and large quantities of flue gas, 'Proceedings of the Combustion Institute', Vol. 28, pp. 1315–1321.

[114] Weber, R., Verlaan, A. L., Orsino, S. and Lallemant, N. (1999), 'On emerging furnace design methodology that provides substantial energy savings and drastic reductions in CO_2, CO and NO_x emissions', *Journal of the Institute of Energy* **72**, 77–83.

[115] Westblom, U. and Aldén, M. (1989), 'Simultaneous multiple species detection in a flame using laser-induced fluorescence', *Applied Optics* **28**(13), 2592–2599.

[116] Westbrook, C. K. and Dryer, F. L. (1984), 'Chemical kinetic modeling of hydrocarbon combustion', *Progress in Energy Combustion and Science* **10**, 1–57.

[117] Williams, F. A. (1985), *Combustion Theory*, 2nd Edn, The Benjamin/Cummings Publishing Company, Inc.

[118] Wünning, J. A. and Wünning, J. G. (1997), 'Flameless oxidation to reduce thermal NO-formation', *Progress in Energy Combustion and Science* **23**, 81–94.

Appendix A

Flame Calculations

This appendix describes the flame calculations referred to throughout the thesis in greater detail. For all calculations, the GRI-Mech 3.0 mechanism is used.

A.1 Nonpremixed Flames

For nonpremixed flames, the OPPDIF code of the CHEMKIN (version 3.6.2) package is used. OPPDIF is used for computing temperature and species concentration for opposed-flow diffusion flames. The OPPDIF configuration (Figure A.1) consists of two facing nozzles (one fuel stream, one oxidant stream) which produce an axisymmetric, one-dimensional flow. The imposed strain rate at the stagnation plane is dependent on the stream velocity and the separation.

The OPPDIF configuration, which simulates opposed-flow laminar diffusion flames, is clearly different to the parallel-flow turbulent flames investigated in this study. Nevertheless, the results from OPPDIF are still closely related to nonpremixed jet flames. The opposed-flow geometry is better suited for simplification of the steady state numerical simulations. Changing the strain rate is somewhat equivalent to the effects of turbulence. It is important to recognise the different geometry between the two configurations however.

In the OPPDIF configuration, the strain rate is not defined at a single point as is the case in some other opposed-flow calculations [98]. Determination of a char-

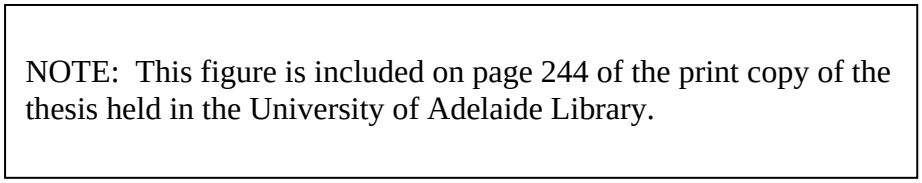

Figure A.1: Schematic representation of the axisymmetric opposed-flow configuration [98].

Oxidant	3% O_2	9% O_2
O_2	0.03	0.09
N_2	0.84	0.78
H_2O	0.10	0.10
CO_2	0.03	0.03

Table A.1: Oxidant (coflow) stream composition (molar basis). Temperature: 1100K.

acteristic strain rate in the OPPDIF configuration must therefore be determined from the velocity profile [98]. The strain rate estimates presented in this work are obtained from the OPPDIF post-processor output file, which gives the average normal strain rate.

For calculations involving the coflow from the JHC burner, the oxidant stream temperature used is 1100K. The oxidant stream was presented in Table 3.5, and the major species composition is re-iterated in Table A.1.

A.2 Number Density

The experimental measurements yield the number density of the species. To determine the number density from the flame calculations the ideal gas law is used;

$$PV = NRT \tag{A.1}$$

Where;
P is the pressure (Pa)
V is the volume (m^3)
N is the number of molecules (mol)
R is the universal gas constant (8.314 J/mol/K)
T is the absolute temperature (K)
A is Avogadro's constant (6.022×10^{23} mol^{-1})

Rearranging equation A.1 to yield the number density ($n = N/V$);

$$\begin{aligned} n &= \frac{P}{R \cdot T} \quad \left(\frac{\text{mol}}{\text{m}^3}\right) \\ &= \frac{A \cdot P}{R \cdot T} \quad \left(\frac{\text{molecules}}{\text{m}^3}\right) \\ &= \frac{A \cdot P}{100^3 \cdot R \cdot T} \quad \left(\frac{\text{molecules}}{\text{cm}^3}\right) \end{aligned}$$

For atmospheric pressure ($P = 101.325\text{kPa}$);

$$n = \frac{7.339 \times 10^{21}}{T} \quad \left(\frac{\text{molecules}}{\text{cm}^3}\right) \tag{A.2}$$

Equation A.2 is for the total number density. The number density of species i, with mole fraction X_i, is;

$$n_i = X_i \cdot \frac{7.339 \times 10^{21}}{T} \quad \left(\frac{\text{molecules}}{\text{cm}^3}\right) \tag{A.3}$$

A.3 Mixture Fraction

Since the coflow oxidant stream consists of combustion products (H_2O and CO_2), the standard definition of mixture fraction is not appropriately defined for calculations based on the mass fraction of H & C (hydrogen & carbon) atoms. To compensate for this, a normalised mixture fraction (ξ^*) is defined based on the mixture fraction found from the calculations (ξ) such that;

$$\xi^* = \frac{\xi - \xi_{oxi}}{\xi_{fuel} - \xi_{oxi}} \tag{A.4}$$

Where ξ_{fuel} & ξ_{oxi} refer to the standard definition of mixture fraction at the fuel and oxidant stream boundaries, respectively.

Key Parameters	Figures 3.25, 3.26 & 3.27	Figure 4.3	Figures 4.10, 4.11 & 7.1	Figures 6.14, 6.15, 6.16, & 7.6
FUEL	C_2H_4: 0.5, H_2: 0.5	Table A.3	CH_4: 0.5, H_2: 0.5	Various
TFUE	300K	300K	300K	300K
VFUE	10, 30, 100, & 500cm/s	50 cm/s	2–500 cm/s	60 cm/s
OXID	Table A.1	Table A.1	Table A.1	Table A.1 & 21% O_2/79% N_2
TOXI	1100K	1100K	1100K	1100K
VOXI	10, 30, 100, & 500cm/s	50 cm/s	4–1000 cm/s	60 cm/s
XEND	2 cm	1 cm	6 cm	2 cm
GRAD	0.3	0.2	0.5	0.3
CURV	0.5	0.5	0.5	0.5
ATOL	1E-6	1E-6	1E-6	1E-6
RTOL	1E-3	1E-3	1E-3	1E-3
ATIM	1E-6	1E-6	1E-6	1E-6
RTIM	1E-3	1E-3	1E-3	1E-3
Diffusion	MIX	MIX	MIX	MULT

Table A.2: Key solution parameters for OPPDIF calculations

A.4 OPPDIF Calculation Parameters

Table A.2 presents the key parameters used for the OPPDIF calculations. Further details of the particular calculations are outlined in subsequent sections. For all cases the pressure is 1 atmosphere and the energy equation is solved.

A.5 Figure 3.25 & 3.26

Figures 3.25 & 3.26 show the calculated Rayleigh cross-section, plotted against either axial distance, or the dimensionless temperature (τ, equation 3.19). The Rayleigh cross-section is determined from major species concentration from OPPDIF calculations. The species considered are; CH_4, C_2H_4, C_3H_8, H_2, N_2, O_2, CO, CO_2, OH & H_2O.

The Rayleigh cross-section is calculated for all of the experimental conditions. Figures 3.25 & 3.26 only present the results for the C_2H_4/H_2, 3% O_2 flame. Table A.2 lists the key solution parameters.

A.6 Figure 3.27

Figure 3.27 shows the calculated OH quenching rate determined from major species concentrations from OPPDIF calculations. The species considered are; OH, N_2, H_2O, CO_2, O_2, CO & H_2.

The OH quenching rate is calculated for all of the experimental conditions. Figure 3.27 only presents the results for the C_2H_4/H_2, 3% O_2 flame. Table A.2 lists the key solution parameters.

Figure 3.27 incorporates the quenching rate with the OH number density, which is found using equation A.3.

A.7 Figure 4.3

Figure 4.3 shows the effect of partial premixing on the peak H_2CO concentration. It consists of a series of nonpremixed flames at various levels of partial premixing and also at premixed conditions.

OPPDIF calculations

Table A.3 shows the fuel stream composition for various fuel-stream equivalence ratios (for partial premixing with air). Each fuel composition in Table A.3 is calculated at the two O_2 levels, with the oxidant stream composition shown in Table A.1. Table A.2 lists the key solution parameters.

Fuel	Φ=3	Φ=6	Φ=12	Φ=24	Φ=∞
CH_4	1	1	1	1	1
H_2	1	1	1	1	1
O_2	0.836	0.418	0.209	0.100	0
N_2	3.144	1.572	0.786	0.377	0

Table A.3: Fuel stream composition (molar basis) for Figure 4.3

PREMIX calculations

At stoichiometric ($\Phi = 1$) mixing with air, PREMIX is used to find the peak H_2CO concentration. The reactant species used are; CH_4=1, H_2=1, O_2=2.5, N_2=9.409 (molar basis). Initial reactant temperature of 400K is assumed. The flame is freely propagating and the energy equation is solved. Solution parameters are: `GRAD`=0.3, `CURV`=0.5, `ATOL`=1E-9, `RTOL`=1E-4, `ATIM`=1E-5, `RTIM`=1E-5.

A.8 Figures 4.10, 4.11 & 7.1

Figure 4.10 shows the effect of imposed strain rate on the peak OH number density, calculated using OPPDIF. A separate run is used for each strain rate, with each run having a different velocity of the fuel and oxidant streams. To ensure the flame front is not affected by the boundary, the oxidant stream velocity is double the fuel velocity. To reduce computational effort, each run is restarted from the adjacent velocity case, starting from v_{fue}=20cm/s (v_{oxi}=40cm/s). From this starting run, the velocity is both increased (in 9 increments up to v_{fue}=500cm/s) and decreased (in 12 increments down to v_{fue}=2cm/s). As the velocity is decreased, the grid is regridded to 25 points after each restart.

Table A.2 lists the key solution parameters. Thermal diffusion effects are included, and in general, mixture averaged transport is used. Some runs were repeated with multi-component transport to confirm that the computationally easier mixture average transport did not introduce perceivable differences.

For generating Figure 4.10, the strain rate is obtained from the OPPDIF post-processor output file. From the post-processor output, the peak OH concentration is found for each of the runs. For the peak OH concentration (mole fraction) the

number density is found using equation A.3.

Figures 4.11 & 7.1 use the same series of calculations as for Figure 4.10, but plot different species from the post-processor output. For Figure 4.11 the peak H_2CO concentration is used. Again, with the strain rate from the post-processor output file. At the location of the peak H_2CO concentration the corresponding O_2 concentration is found to generate Figure 7.1.

A.9 Figures 6.14, 6.15, 6.16 & 7.6

Figures 6.14, 6.15, 6.16 & 7.6 show selected species concentrations for a single fixed velocity case (v_{fue}=v_{oxi}=60 cm/s). Three fuels are considered for Figures 6.14, 6.15 & 6.16; CH_4/H_2, C_2H_4/H_2 & C_3H_8/H_2 in an equal volumetric ratio of hydrocarbon to hydrogen. For Figure 7.6 the fuels are; CH_4, C_2H_4 & C_3H_8.

For the diluted O_2 cases, the oxidant stream composition is from Table A.1 at a temperature of 1100K. For the cold (standard air) the temperature is 300K, and air is assumed 21% O_2 & 79% N_2.

Table A.2 lists the key solution parameters.

A.10 Figures 7.2, 7.3, 7.4 & 7.4

Figures 7.2, 7.3, 7.4 & 7.4 show relevant species and reaction rates for determination of the production of H_2CO. These figures are generated from four selected cases from the runs described in §A.8. For both the 3% & 9% O_2 cases, two velocity runs were chosen, namely; v_{fue}=30cm/s (v_{oxi}=60cm/s) and v_{fue}=300cm/s (v_{oxi}=600cm/s).

From the selected runs, the OPPDIF post-processor is used to generate the production rate for H_2CO and also O. Reaction rates less than 1% are excluded from the post-processor output files.

Oxidant	Fuel	C_2H_4	H_2	N_2	O_2	H_2O	CO_2
3% O_2 (1100K)	C_2H_4	1	0	84.00	3.0	10.00	3.00
	C_2H_4/H_2	1	1	98.00	3.5	11.67	3.50
	C_2H_4/air	1	0	68.73	3.0	7.90	2.37
	C_2H_4/N_2	1	0	87.00	3.0	10.00	3.00
9% O_2 (1100K)	C_2H_4	1	0	26.00	3.0	3.33	1.00
	C_2H_4/H_2	1	1	30.33	3.5	3.89	1.17
	C_2H_4/air	1	0	22.91	3.0	2.63	0.79
	C_2H_4/N_2	1	0	29.00	3.0	3.33	1.00
15% O_2 (1100K)	C_2H_4	1	0	17.00	3.0	0	0
	C_2H_4/H_2	1	1	19.83	3.5	0	0
	C_2H_4/air	1	0	16.60	3.0	0	0
	C_2H_4/N_2	1	0	20.00	3.0	0	0
21% O_2 (1100K)	C_2H_4	1	0	11.29	3.0	0	0
	C_2H_4/H_2	1	1	13.17	3.5	0	0
	C_2H_4/air	1	0	11.29	3.0	0	0
	C_2H_4/N_2	1	0	14.29	3.0	0	0

Table A.4: Reactant composition for PREMIX calculations of laminar flame speed. Note that the fuel and oxidant are not applicable for these premixed calculations, and are included only for designation of the nonpremixed flame conditions.

A.11 Table 7.1

Table 7.1 presents laminar flame speed calculations from the PREMIX code of CHEMKIN (version 3.6.2). The laminar flame speed is found for a stoichiometric mixture for each fuel type and oxidant stream composition. The premixed composition and temperature for each of the flame cases is shown in Table A.4.

To determine the laminar flame speed, the premixed flame is solved as a freely propagating flame. The energy equation is solved. The velocity at the base of this flame represents the laminar flame speed.

The computational domain extends from X=–0.5cm to 10cm, with convergence criteria of `GRAD`=0.5 & `CURV`=0.5, `ATOL`=1E-8, `RTOL`=1E-6, `ATIM`=1E-6, `RTIM`=1E-6. Multi-component transport with thermal diffusion is used.

Appendix B

OH-LIF Linearity

This appendix demonstrates the linearity of the OH laser induced fluorescence measurements (OH-LIF). To test for linearity, a separate experiment was conducted. The same Lambda-Physik ScanMate 2E dye laser, pumped with a Quantel BrilliantB/Twins Nd:YAG, (§3.3.2) was used in both campaigns.

To simplify the experimental setup, the beam leaving the laser (after the Pellin-Broca array) is only passed through a single spherical lens (f=1000mm). A simple laminar partially-premixed methane/air flame located at the focal point provides a stable source of OH.

To investigate the dependence of the OH-LIF on the spectral intensity, the laser power is adjusted. To decrease the laser energy without affecting the beam profile and characteristics, the doubling crystals are misaligned to reduce the ultra-violet (UV) emission. The linewidth of the UV laser pulse was measured to verify that it is consistent with the turbulent flame measurements (i.e. $\Delta\nu = 0.5\text{cm}^{-1}$).

At each laser energy, the OH signal is averaged from the maximum in each of 100 images. Figure B.1 shows the dependence of the maximum OH-LIF signal from the flame for various laser energies.

From Figure B.1 it appears that the OH-LIF is linear with laser energy up to around 1 mJ/pulse. Even at 1 mJ/pulse there is some slight non-linearity, but this is quite minor. The beam diameter (round because of the spherical lens used) has been measured to be 1mm (both from burns to photosensitive paper and from

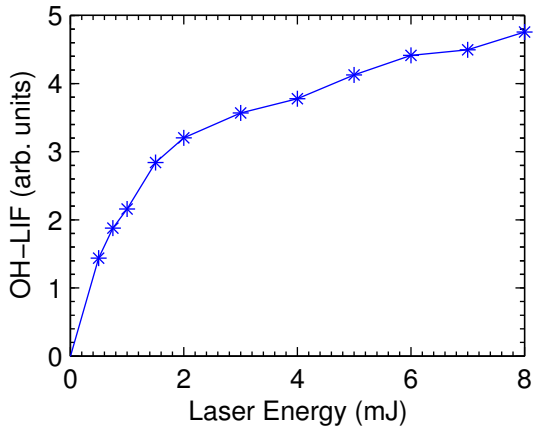

Figure B.1: OH-LIF dependence on laser energy

scaling from the images themselves). The OH-LIF is therefore considered linear up to $\sim$1.2 mJ/mm^2.

For the turbulent flame measurements, the laser energy through the probe volume was 2 mJ/pulse. The laser sheet was 12mm in height. The in-plane resolution of the OH imaging was 160µm. Burns from photosensitive paper suggest that the sheet thickness was greater than this, but accurate determination from the burns was not possible. Using 160µm as the sheet thickness is an under-estimate, which will subsequently over-estimate the flux. Assuming a 160µm sheet thickness, the fluence in the turbulent flame images is $\sim$1 mJ/mm^2. Since this fluence is less than that considered linear (1.2 mJ/mm^2) the measurements are therefore within the linear regime.

Appendix C

Publications

Publications arising from this thesis

Medwell, P. R., Kalt, P. A. M. and Dally, B. B. (2005), Effect of Fuel Dilution on Jet Flames in a Heated and Diluted Co-flow, '5th Asia-Pacific Conference on Combustion', The University of Adelaide, Adelaide, Australia, pp. 325–328.

Medwell, P. R., Kalt, P. A. M. and Dally, B. B. (2005), Effect of Reynolds number on the Spatial Distribution of OH and Formaldehyde in Jet Flames in a Heated and Diluted Co-flow, '5th Asia-Pacific Conference on Combustion', The University of Adelaide, Adelaide, Australia, pp. 381–384.

Medwell, P. R., Kalt, P. A. M. and Dally, B. B. (2005), Quantification of OH-LIF in Jet Diffusion Flames, 'Fourth Australian Conference on Laser Diagnostics in Fluid Mechanics and Combustion', The University of Adelaide, South Australia, Australia, pp. 105–108.

Medwell, P. R., Kalt, P. A. M. and Dally, B. B. (2007), 'Simultaneous imaging of OH, formaldehyde, and temperature of turbulent nonpremixed jet flames in a heated and diluted coflow', *Combustion and Flame* **148**, 48–61.

Medwell, P. R., Kalt, P. A. M. and Dally, B. B. (2007), Structure of Ethylene Based Nonpremixed Flames Stabilised on a JHC Burner, '6th Asia-Pacific Conference on Combustion', Nagoya Congress Center, Nagoya, Japan, pp. 452–455.

Medwell, P. R., Kalt, P. A. M. and Dally, B. B. (2007), 'Imaging of Diluted Turbulent Ethylene Flames Stabilised on a Jet in Hot Coflow (JHC) Burner', *Combustion and Flame*. IN PRESS.

Medwell, P. R., Kalt, P. A. M. and Dally, B. B. (2007), Influence of Fuel Type on Turbulent Nonpremixed Jet Flames Under MILD Combustion Conditions, '16$^{\text{th}}$ Australasian Fluid Mechanics Conference', Crown Plaza, Gold Coast, Australia. SUBMITTED.

Medwell, P. R., Kalt, P. A. M. and Dally, B. B. (2007), Influence of Fuel Composition on the MILD Combustion Reaction Zone Structure in a JHC Burner, 'Proceedings of the Australian Combustion Symposium', University of Sydney, Australia. SUBMITTED.

Medwell, P. R., Kalt, P. A. M. and Dally, B. B. (2007), The Role of Hydrogen Addition on the Structure and Stability of Hydrocarbon Flames in a JHC burner, '7$^{\text{th}}$ High Temperature Air Combustion and Gasification International Symposium', Phuket, Thailand. ACCEPTED.

Quod Erat Demonstrandum ✷—

PERMISSIONS TO INCLUDE FIGURES

Fig. 2.1
Mi, J., Nobes, D.S. and Nathan, G..J. (2001), 'Influence of jet exit conditions on the passive scalar field of an axisymmetric free jet', Journal of Fluid Mechanics, 432, 91-125

Permission to include figure in electronic thesis granted by Cambridge University Press.

Fig. 2.2
Westbrook, C.K. and Dryer, F.L. (1984), 'Chemical kinetic modelling of hydrocarbon combustion', Progress in Energy and Combustion Science, 10, 1-57

Reprinted with permission from Elsevier

Fig. 2.3
Refael, S. and Sher, E. (1989), 'Reaction kinetics of hydrogen-enriched Methane-Air and Propane-Air Flames', Combustion and Flame 78, 326-338

Reprinted with permission from Elsevier

Fig. 2.11
Wunning, J.A. and Wunning, J.G. (1997), 'Flameless oxidation to reduce thermal NO-formation', Progress in Energy and Combustion Science 23, 81-95

Reprinted with permission from Elsevier

Fig. 2.12
Choi, G.-M. and Katuski, M. (2001), 'Advanced low No[subscript x] combustion using highly preheated air', Energy Conversion and Management 42, 639-652

Reprinted with permission from Elsevier

Fig. 3.17
Emery, C.D., Overway, K.S., Bouwens, R.J. and Polik, W.F. (1995), 'Dispersed fluorescence spectroscopy of excited rovibrational states in S[subscript O] formaldehyde', Journal of Chemical Physics 103 (13), 5279-5289

Reprinted with permission from American Institute of Physics